Powder Technology 428 (2023) 118853

Contents lists available at ScienceDirect

Powder Technology

journal homepage: www.journals.elsevier.com/powder-technology

Feasibility of using high-volume pozzolanic fillers to develop sustainable engineered cementitious composites (ECC)

Minghu Zhang [a], Xuezhen Zhu [a], Sukhoon Pyo [b], Yuanxia Yang [a,**], Baoju Liu [a,c,*], Jinyan Shi [a]

[a] School of Civil Engineering, Central South University, Changsha 410075, China
[b] Department of Urban and Environmental Engineering, Ulsan National Institute of Science and Technology (UNIST), 50 UNIST-gil, Ulju-gun, Ulsan, Republic of Korea
[c] National Engineering Research Center of High-speed Railway Construction Technology, Changsha 410075, China

HIGHLIGHTS

- A high-volume SCM ECC (HSECC) containing DP is prepared.
- The mechanical properties and volume stability of HSECC are investigated.
- Incorporating 10%–30% DP significantly increases tensile ductility of HSECC.

GRAPHICAL ABSTRACT

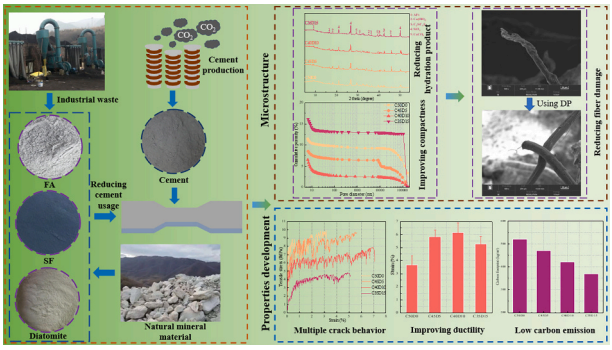

ARTICLE INFO

Keywords:
Engineered cementitious composites
High-volume
Supplementary cementitious material
Strain capacity
Environmental assessment

ABSTRACT

To decrease the environmental load caused by the cement production, high volume of supplementary cementitious materials (SCMs) are adopted to prepare the engineered cementitious composites (ECC). This work prepares an eco-friendly ECC mixed with high-volume SCM (HSECC) by incorporating silica fume, fly ash and diatomite powder (DP) to reduce the cement dosage. The mechanical properties, volume deformation, microstructure, and environmental benefit of HSECC are investigated. Experimental results present that with increasing the DP replacement ratio, the compressive strength of the HSECC gradually reduces, whereas its autogenous shrinkage deformation increases. Furthermore, with increasing the DP content, tensile strain capacity and crack number of HSECC increase, but the tensile strength reduces. The tensile strain capacity of HSECC containing 20% DP increases by 67.8% compared with the HSECC without DP. Utilizing DP to replace the cement reduces the amount of hydration production, but it optimizes the pore structure of sample because of the filling effect, pozzolanic reaction and internal curing effect of DP. Moreover, the HSECC containing DP has a lower carbon emission and cost compared to the HSECC without DP. This study gives a new strategy and theoretical support for producing the eco-friendly high-ductility ECC.

* Corresponding author at: School of Civil Engineering, Central South University, Changsha 410075, China.
** Corresponding author.
E-mail addresses: 562849410@qq.com (Y. Yang), bjliu@csu.edu.cn (B. Liu).

https://doi.org/10.1016/j.powtec.2023.118853
Received 19 March 2023; Received in revised form 6 July 2023; Accepted 27 July 2023
Available online 29 July 2023

1. Introduction

Currently, concrete is the most consumed construction material. Due to the high demand for concrete, >4 billion tons of cement are used globally every year. Lots of cement production triggers serious carbon emissions and consumption of non-renewable resources. Reducing cement dosage in concrete is considered as one of the solutions to reduce environmental impact of building materials. Incorporating high volume of supplementary cementitious materials (SCMs) to replace cement is recognized by many researchers as an effective strategy to decrease carbon emissions and improve some performances of concrete materials [1,2].

Over the years, various industrial waste, waste incineration bottom ash or natural pozzolan materials have been used as the SCMs to produce the sustainable concrete [3–5]. Du and Tan found that the incorporation of 60% glass powder to replace cement significantly improved the impermeability of concrete [3]. Liu et al. elaborated that although utilizing natural pozzolan instead of 50% cement decreased the compressive strength of concrete by 15%, it significantly decreased the environmental load of concrete [4]. Hamada et al. found that the incorporation of 0–80% palm oil fuel ash instead of cement reduced the drying shrinkage and water absorption of concrete [5]. Therefore, incorporating high-volume SCM to replace cement positively affects the properties development of eco-friendly concrete. However, the service environment of concrete is very complex and harsh in actual engineering [6], such as seawater erosion and impact damage. Apart from the policies restrictions of saving resources and low carbon emissions, the brittle failure of traditional concrete also restricts its application range of engineering structure in severe environment [7]. In recent years, with the advancement of fiber preparation technology, the high-ductility fiber-reinforced concrete also has greatly developed, among which the engineered cementitious composites (ECC) have received the attention of researchers due to its excellent ductility and durability [8].

The ECC is proposed by Victor C. Li and has an excellent ductility and durability. Its appearance greatly solves the brittleness and easy cracking problem of traditional cement-based material. According to the design of fracture mechanics theory, ECC exhibits multi-crack cracking performance under the tensile loading [9], and its tensile strain capacity can reach 2%–9% [10]. Meanwhile, the tensile crack width of ECC is usually <100 μm [11], which is very beneficial to improve the service life of concrete structural components in complex environments. Owing to its excellent tensile ductility and crack control capabilities, ECC has been currently applied in practical projects, such as bridge deck repair, dam reconstruction, and beam-column joints/beams/beam-column mid-joints [12]. However, similar to traditional concrete, the high cement usage in the ECC also results in a high carbon emission [13]. Therefore, while improving the performance of ECC, it is necessary to further reduce the economic and environmental burdens of ECC.

Over the years, researchers have prepared different types of eco-friendly ECC by incorporating high volume of SCM instead of cement. Zhu et al. used the high-volume fly ash, ground granulated blast furnace slag and silica fume to replace cement in ECC [14]. Results reported that the incorporation of high volume of SCMs resulted in reducing by 80% of cement dosage and improving the compressive strength and ductility of ECC containing high-volume SCM (HSECC) [14]. Şahmaran and Li found that incorporating fly ash positively affected the development of tensile strain capacity of ECC, and this mixture (cement/fly ash:1.2) has been widely used [15]. Meanwhile, Ma et al. said that with further increasing the content of fly ash, the tensile strain capacity of HSECC gradually increased [16]. Wu et al. reduced the cement dosage of HSECC to 42% by using recycled brick powder and silica fume as ternary binders, and the strain capacity of HSECC was improved with the growth of SCM content [17]. Zhang et al. studied the mechanical property of HSECC using cement, fly ash, silica fume and rice husk ash [18]. The results revealed that the growth of SCM replacement ratio resulted in increasing the tensile strain and reducing the carbon emissions of HSECC. Therefore, the use of high volume of SCM (e.g., slag, fly ash, and silica fume) as the binder is an effective way to enhance ductility and achieve the low carbon emission of HSECC.

Due to the green transition of heavy industry, some SCMs (fly ash and slag) gradually have the issue of insufficient supply and price rise. In such case, finding potential SCMs instead of traditional SCMs is necessary and thus solves the problem of insufficient supply of traditional SCM. Diatomite is a natural material formed from the remains of diatoms. Diatomite powder (DP) contains 86%–94% silicon dioxide and is identified as the pozzolanic material [19,20]. Literatures showed that utilizing DP to replace cement positively affected the development of the mechanical properties of cement-based material [21,22]. Meanwhile, there are 920 million tons of DP in the world, which has rich diatomite reserves. Therefore, it is an acceptable strategy to consider the DP as an alternative SCM, which can solve the demand for the high volume of SCM in ECC. Meanwhile, diatomite has a fine particle size, and incorporating an appropriate amount of diatomite as SCMs can broaden the particle size distribution range of powder materials and fill the pore, thereby increasing the wet packing density and reducing the porosity of solid phase [23–25]. Therefore, incorporating DP may be beneficial to the improvement of mechanical properties of HSECC.

As mentioned above, there are currently insufficient reserves of some

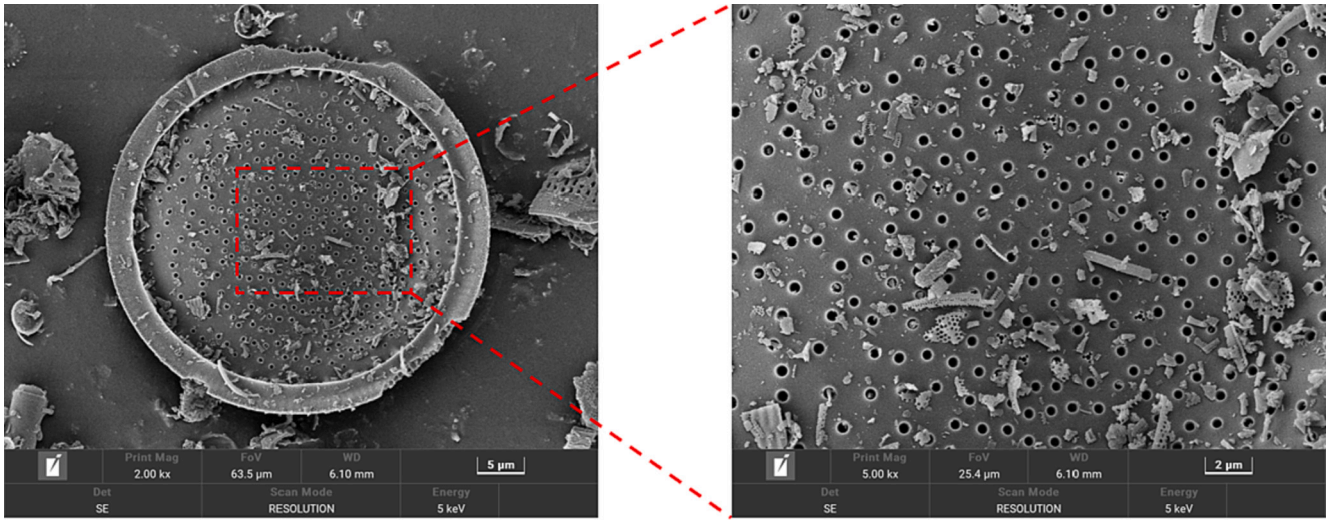

Fig. 1. SEM image of DP particle.

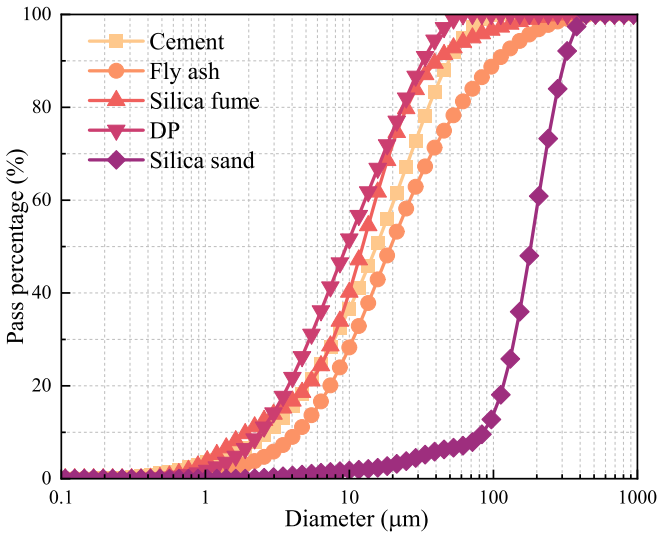

Fig. 2. Particle gradation curve of raw material.

SCMs. In order to achieve the goal of reducing the environmental impact of ECC, this study utilizes various SCMs (e.g., fly ash, silica fume, and DP) to prepare a high-ductility sustainable HSECC, and the mechanical properties, volume deformation, and microstructure of HSECC are also systematically characterized. Furthermore, the economic and environmental benefits of ECC containing a large amount of SCMs are evaluated. This study expands the application range of DP in cement-based materials, and gives a theoretical guidance for the application of high volume of SCM in ECC system.

2. Experimental programs

2.1. Materials

Ordinary Portland cement (42.5 grade), fly ash, silica fume, DP, silica sand, polyethylene (PE) fiber, water, and superplasticizer (SP) are used to prepare HSECC mixture. DP is purchased from Jilin Yuantong Mining Co., Ltd., and its median particle size and maximum particle size of DP are 9.53 and 64.51 μm, respectively. SiO_2 is the main chemical component of DP, accounting for about 94%. The scanning electron microscope (SEM) image of DP presents that it is a porous structure (See Fig. 1). The fine aggregate is silica sand with a particle size of 120–180 μm. The particle gradation curves of cementitious material and fine aggregate are shown in Fig. 2. The PE fiber has an excellent tensile strength and is often adopted to attain the high strain-hardening behavior of ECC. The length, diameter, and tensile strength of PE fiber are 18 mm, 15.6 μm, and 3.98 GPa, respectively. Moreover, SP is used to modify the fluidity of HSECC mixture, and its solid content is around 40%. Tap water is utilized as the mixing water.

2.2. Mix proportions

Table 1 gives that the mix proportion of HSECC. The DP replaces cement by the same weight, and its replacement ratio contains 0%, 10%, 20%, and 30%. The HSECC mixture without DP (C50D0) is considered as the reference group. In the HSECC mixture, the volume content of fiber and water-binder ratio are designed at 2% and 0.2, respectively. Besides, the fluidity of all mixtures is modified to 120–140 mm to ensure good dispersion of fibers [8,13].

2.3. Mixing procedure

During the stirring process, a planetary mortar with 5 L capacity was adopted to prepare the mixture. First, all solid materials including cement, fly ash, silica fume, DP, and sand were poured into the mixer and stirred at 140 r/min for 2 min. Subsequently, pour water and SP together into the mixer and stir at 140 r/min for 4 min. Fibers were slowly added to the mixture and stirred at 140 r/min for 4 min. And then, switch the stirring speed to 285 r/min and stir the mixture for 6 min. Next, the HSECC mixture was cast into the molds and cured at 20 °C for 24 h. After demolding, all specimens were placed into the standard curing room (20 ± 2 °C and relative humidity >95%) for curing until the test age.

3. Experimental methods

3.1. Compressive strength

Based on the ASTM C109, six cubic specimens with the side length of 40 mm are prepared to measure the compressive strength of HSECC in each mixture. This test is carried out by using a 300 kN testing machine with loading speed of 2400 N/s.

Table 1
Mix proportion of HSECC with DP (wt%).

Mixture	Cement	DP	Fly ash	Silica fume	Sand	Water	SP	Fiber (vol%)
C50D0	0.5	0	0.45	0.05	0.35	0.2	0.006	2
C45D5	0.45	0.05	0.45	0.05	0.35	0.2	0.011	2
C40D10	0.4	0.1	0.45	0.05	0.35	0.2	0.038	2
C35D15	0.35	0.15	0.45	0.05	0.35	0.2	0.061	2

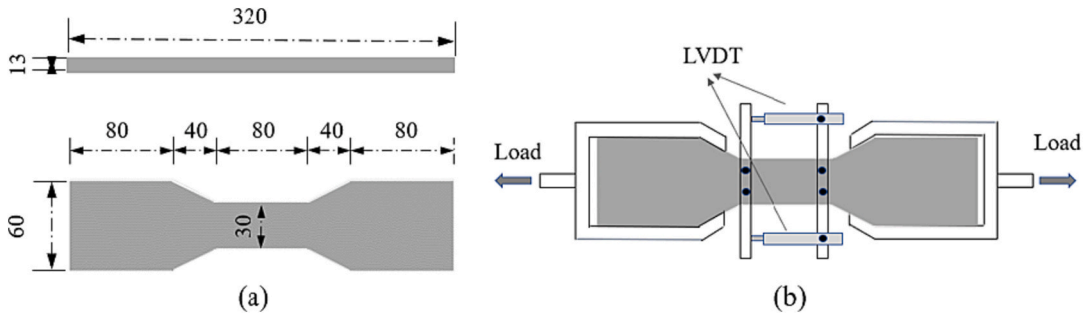

Fig. 3. Uniaxial tensile test. (a) Dog-bone specimen and (b) Tensile device.

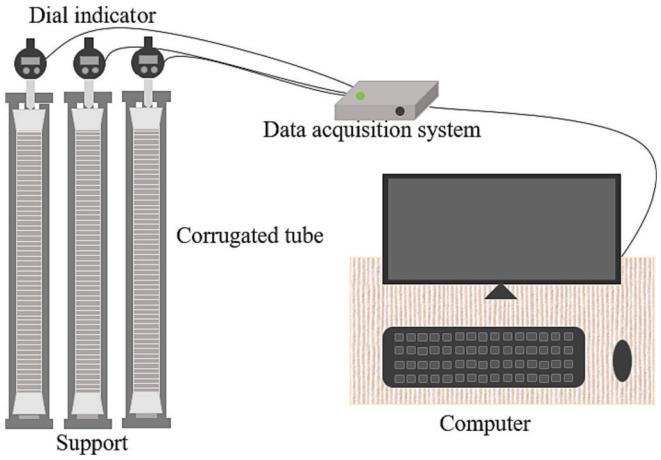

Fig. 4. Autogenous shrinkage test of HSECC paste.

3.2. Uniaxial tensile test

The dog-bone specimen is prepared to measure the stress-strain curve of HSECC, and its specific shape is plotted in Fig. 3(a). During the tensile test, the loading rate of HSECC sets 0.5 mm/min. The axial deformation in the central rectangular area (80 mm) of the dog-bone specimen is regarded as the uniaxial tensile displacement, which is monitored by the linear variable displacement transducer (LVDT). The uniaxial tensile test is illustrated in Fig. 3(b). Six dog-bone specimens are prepared for each HSECC group to ensure the reliability of experimental results.

3.3. Autogenous shrinkage

According to ASTM C1698, the fresh HSECC paste is casted into the corrugated plastic tubes before it is sealed with the plastic plug. The test equipment of autogenous shrinkage is presented in Fig. 4. The end of corrugated plastic tube connects with a dial indicator to gather the deformation of plastic tube, meanwhile, a set of data acquisition system regularly collects the value change of the dial indicator. When the paste reaches the final setting status, it is placed on the support and measure the shrinkage deformation of the corrugated plastic tube by the dial indicator until 14 d. Three corrugated tubes containing paste are prepared for each mixture.

3.4. Microstructure

An X-ray diffraction (XRD) test is used to evaluate the phase composition of the paste at the age of 28 d. During the test, the 2-theta scanning angle is 5–55° with a rate of 10°/min. In addition, fourier transform infra-red (FT-IR) spectra test is carried out to characterize the changes of functional groups of the pastes with different DP contents, and its wavenumber used in this study ranges from 500 to 4000 cm^{-1}. During the preparation of sample, the paste at the age of 28 d is soaked in isopropanol for a week and then crushed into the powder. The powder samples are dried 7 d in vacuum before the experiment started.

The thermogravimetric (TG) test of HSECC paste mixed with DP is performed to evaluate the reaction degree and $Ca(OH)_2$ content of the sample. Under the N_2 environment, the sample is gradually heated from 30 to 1000 °C at 10 °C/min. Non-evaporative water content often reflects the degree of reaction of binder. Based on the literature [26,27], the non-evaporative water and $Ca(OH)_2$ contents are calculated according to Eqs. (1) and (2).

Table 2
Economic and environmental indexes of cementitious material.

Material	Cost (USD/ton)	Embodied CO_2 (kg CO_2/kg)	Ref.
Cement	84	0.69	[29]
Fly ash	37.5	0.009	[28]
Silica fume	1050	0.024	[30,31]
DP	10	0.016	[29]

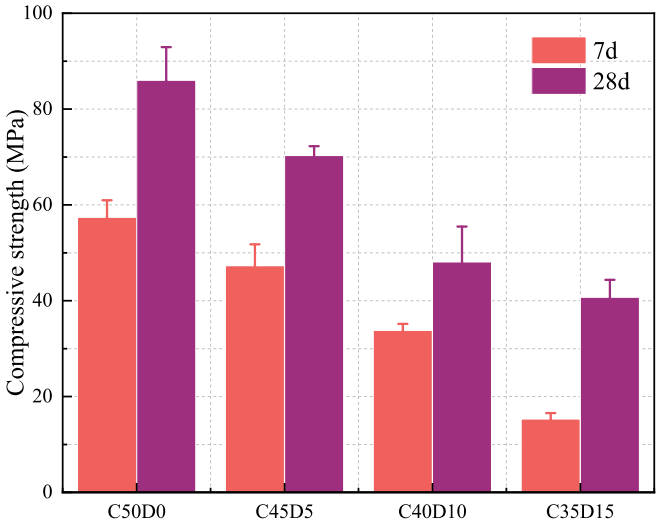

Fig. 5. Compressive strength of HSECC with different DP contents.

$$W_{water} = \left[\frac{m_{105} - m_{950}}{m_{105}} - (f_C \times LOI_C + f_F \times LOI_F + f_S \times LOI_S + f_D \times LOI_D)\right] \times 100\% \quad (1)$$

$$W_{CH} = \left(\frac{m_{400} - m_{500}}{m_{Total}} \times \frac{74}{18} + \frac{m_{500} - m_{780}}{m_{Total}} \times \frac{74}{44}\right) \times 100\% \quad (2)$$

where W_{water} and W_{CH} represent the non-evaporable water and $Ca(OH)_2$ contents, respectively. m_n represents the mass of sample at the specific temperature of n °C. m_{Total} represents the unheated mass of sample. LOI_c, LOI_F, LOI_S, and LOI_D represent the LOI of cement, fly ash, silica fume, and DP, respectively. f_c, f_F, f_S, and f_D represent the mass fraction of cement, fly ash, silica fume, and DP in the cementitious material, respectively.

Furthermore, the pore structure characteristics of HSECC paste containing DP are tested by the mercury intrusion porosimetery (MIP). The test range of pore diameter is 6–174,300 nm, and the sample size is 5–7 mm. SEM test is adopted to observe the microscopic morphology characteristics of the HSECC sample, and its sample is chosen from the dog-bone specimen after the tensile test. Before the SEM test, all samples are sprayed with gold.

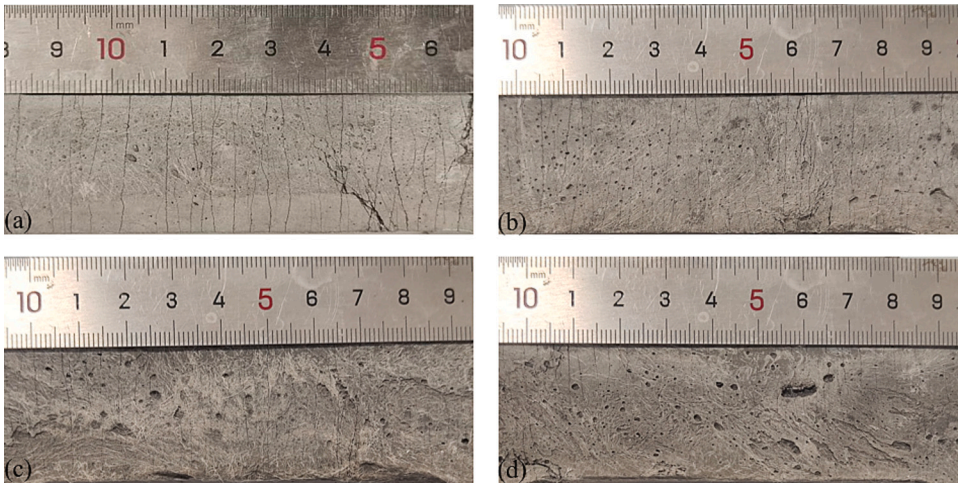

Fig. 6. Multiple cracking behaviors of HSECC with different DP contents. (a) C50D0, (b) C45D5, (c) C40D10, and (d) C35D15.

3.5. Cost and environmental benefits

In recent years, the production of cement is regarded as the important contributor of the greenhouse effect. With the introduction of the concept of sustainable development, researchers increasingly focus on the reduction of carbon emissions from building materials [28]. Additionally, low cost is also an important factor to affect the application of cement-based materials in practical engineering. Therefore, reducing the carbon emissions and costs of cement-based materials are one of the pressing issues in construction industry. It is very necessary to conduct environmental and cost assessments of building materials. The costs and carbon emissions of all cementitious materials for HSECC containing DP are shown in Table 2, and these data are obtained from the other literatures.

4. Result and discussion

4.1. Compressive strength

Fig. 5 shows the compressive strength of HSECC with DP at different curing ages. As the curing age increases, the compressive strength increases, which is due to the continuous hydration of the cementitious material. At the same curing age, incorporating DP results in reducing the compressive strength of HSECC, and the compressive strength of sample gradually decreases with increasing the DP dosage. For example, the 28-d compressive strength of HSECC without DP (C50D0) is 86 MPa, while those of the HSECC with 10%, 20%, 30% DP are 70.3, 48.1, 40.7 MPa, respectively corresponding to approximately 18.26%, 44.07% and 52.7% decrease compared with that of the HSECC without DP. The use of high-volume DP greatly reduces the cement dosage and free water content, which reduces the amount of hydration product of the specimen, thereby decreasing the bonding force at the aggregate/paste interface. Meanwhile, the dilution effect of DP also has a negative effect on the compressive strength development of HSECC containing DP, especially at the high DP content. Therefore, the incorporation of DP results in decreasing the compressive strength of HSECC. Besides, some literature reported that the DP reacted with calcium hydroxide to form C-S-H gel, and its incorporation also results in increasing the wet packing density of solid material, which contributes to improve the compressive strength of sample, but this positive influence of DP might be insufficient [21]. The reduction of compressive strength of sample caused by incorporating DP is also consistent with other published literatures which reported that the incorporation of DP instead of 10%–40% of cement resulted in reducing by 25%–39% of the 28-d compressive strength of mortar [32].

4.2. Tensile stress-strain behavior

Figs. 6 and 7 show the crack characteristics and tensile stress-strain curves of HSECC with different DP dosages. The tensile performance of HSECC containing DP conforms to the typical bilinear tensile stress-strain model of ECC (See Fig. 8) [33]. All HSECC samples exhibit the multiple cracking performance, which corresponds to the excellent strain capacity of the specimens. Meanwhile, almost no large cracks are observed in the HSECC specimens containing different DP contents under the tensile loading, which contributes to improving the service life of concrete structures.

Fig. 9 plots all critical tensile parameters of each HSECC sample including first cracking strength, ultimate tensile strength, strain capacity, crack number, and crack width. It is clearly marked that with increasing DP dosage, the first cracking strength and ultimate tensile strength of HSECC gradually reduce. The first cracking strength and ultimate tensile strength of C35D15 sample are 2.06 and 5.37 MPa, respectively, which decreases by 63.3% and 47.6%, respectively, in comparison with the reference sample (C50D0), respectively. Incorporating DP decreases the amount of hydration products of cement and free water content, thereby decreasing the bonding stress of the fiber/matrix interface. Although incorporating a large amount of DP results in decreasing the ultimate tensile strength of HSECC, it also reduces the cement usage, which is beneficial to prepare the eco-friendly HSECC. Moreover, the ultimate tensile strength of HSECC mixed with 30% DP still is similar to that of polyvinyl alcohol (PVA)-ECC [34,35], which shows that the HSECC with 30% DP still has an enormous potential to apply in the civil engineering.

In terms of the influence of DP content on strain capacity, the strain capacity of HSECC firstly increases and then slightly reduces with increasing the DP replacement ratio. The highest strain capacity of HSECC reaches when the DP content is 20%. Strain capacity increases from 3.67% for C50D0 sample to 6.16% for C40D10 sample, and slightly decreases to 5.27% when the DP content further increases from 20% to 30%. It is worth noting that the strain capacity of C40D10 sample is 67.8% higher than that of C50D0 sample, which illustrates the incorporation of DP has a positive influence on the improvement of tensile ductility of HSECC. The improvement of strain capacity may be because that the incorporation of DP improves the fiber dispersion degree and deteriorates the fracture energy of HSECC matrix. Lei et al. pointed out that the ductility of ECC was closely related to the dispersion degree of fiber [36]. As a material of high specific surface area, DP effectively improves the degree of fiber dispersion [36]. Meanwhile, based on the compressive strength and crack number (Figs. 5 and 9), it deduces that utilizing DP to replace cement may reduce the fracture energy of HSECC

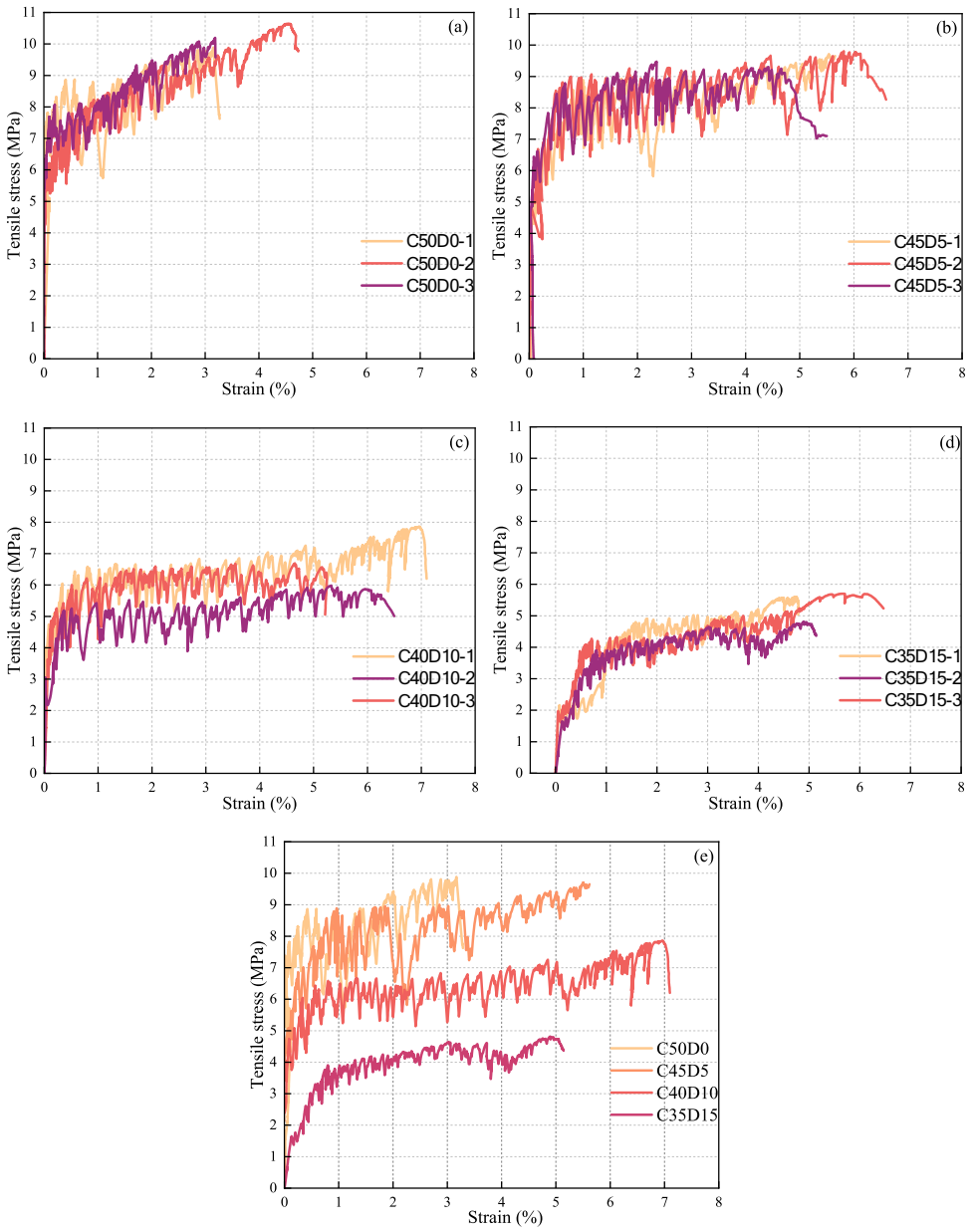

Fig. 7. Tensile stress-strain curves of HSECC with DP. (a) C50D0, (b) C45D5, (c) C40D10, (d) C35D15, and (e) All mixtures.

matrix, so as to reduce the energy requirement for the generation of new crack. However, incorporating excessive DP may make a large amount of water be absorbed by DP, which is not conducive to the compactness of sample and the bonding stress of the fiber/matrix interface, thereby significant reducing the fiber-bridge stress of HSECC sample. Therefore, the strain capacity of HSECC reduces when the DP replacement ratio exceeds 20%. It is interesting that the strain capacity of C35D15 is still 43.6% higher than that of C50D0 sample, implying that the strain capacity of HSECC with 30% DP still reaches hundreds of times that of traditional concrete.

Notably, compared with the HSECC without DP (C50D0), the ultimate tensile strength of HSECC with 10% DP only decreases by 5.7%, but its strain capacity significantly increases by 59.1%. Using a little DP can significantly increase the strain hardening behavior of HSECC beam/plate components while there is a slight tensile strength loss, which is conducive to avoid the occurrence of brittle failure of concrete structure under impact loading.

After the uniaxial tensile test, crack number is counted by visual inspection method, meanwhile, average crack width is calculated. Average crack width is equal to the tensile deformation value in the middle measurement region (80 mm) of the dumbbell specimen divided by the crack number. Finally, Fig. 9 lists the crack characteristics of specimens. All specimens have the multiple cracking pattern behavior, and these average cracks width are narrow (<100 μm). As demonstrated in Fig. 9, the crack number of specimen increases with the increase of DP content up to 20% and then reduces. Additionally, average crack width demonstrates a same change trend as the crack number with the increase of DP content. Among all specimen, C45D5 specimen has the largest crack width, which reaches 95 μm.

4.3. *Autogenous shrinkage*

The autogenous shrinkage of HSECC sample containing DP is shown in Fig. 10. As the DP replacement ratio increases, the autogenous shrinkage value of HSECC significantly increases. The 14-d autogenous shrinkage value of reference specimen (C50D0) is 979 μm/m, while those of the HSECC with 10%, 20%, 30% DP are 2274, 2971, 5143 μm/m, respectively corresponding to 2.32, 3.03 and 5.25 times of the C50D0

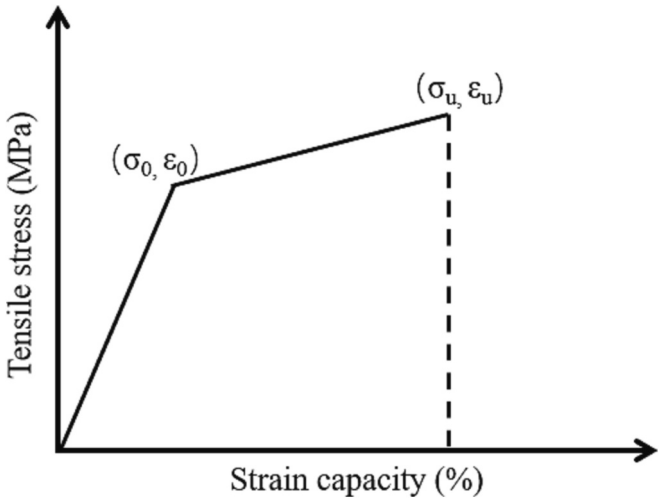

Fig. 8. Typical tensile stress-strain relation model of ECC.

sample. The incorporation of DP reduces the stiffness of HSECC samples, thereby decreasing the resistance of shrinkage deformation [37]. Additionally, the porous DP absorbs a large amount of mixing water, which reduces the effective water-binder ratio in HSECC, resulting in an increase of capillary pressure of HSECC. Although DP releases the absorbed water to suppress autogenous shrinkage during the hydration process, it may not offset the increase of shrinkage deformation of HSECC paste as a result of the reduction of stiffness and effective water-binder ratio of sample. Finally, autogenous shrinkage of HSECC mixture increases with increasing DP replacement ratio. Besides, incorporating finer DP to replace cement may also increase the capillary pressure inside the paste [38,39].

4.4. Microstructure

4.4.1. XRD

Fig. 11 displays the XRD patterns of four specimens at 28 d. The main characteristic peaks of cement clinker (C_2S and C_3S) and hydration products ($Ca(OH)_2$ and AFt) are found in each sample. Meanwhile, the characteristic peaks of SiO_2 can also be observed, which originates from the DP and silica fume in sample. The use of DP does not influence the type of hydration products. However, due to incorporating different DP contents, some peak intensities of each sample are different. As displayed in Fig. 11, the peak intensity of $Ca(OH)_2$ demonstrates a decrease trend with the increase of DP replacement ratio, which mainly is due to the reduction of cement dosage and free water content. Meanwhile, the DP consumes $Ca(OH)_2$ to play its pozzolanic effect under the alkaline environment, which further reduces the amount of $Ca(OH)_2$. Moreover, the peak intensity of C_2S/C_3S gradually increases with increasing the DP replacement ratio. As a porous material, the DP absorbs part of mixing

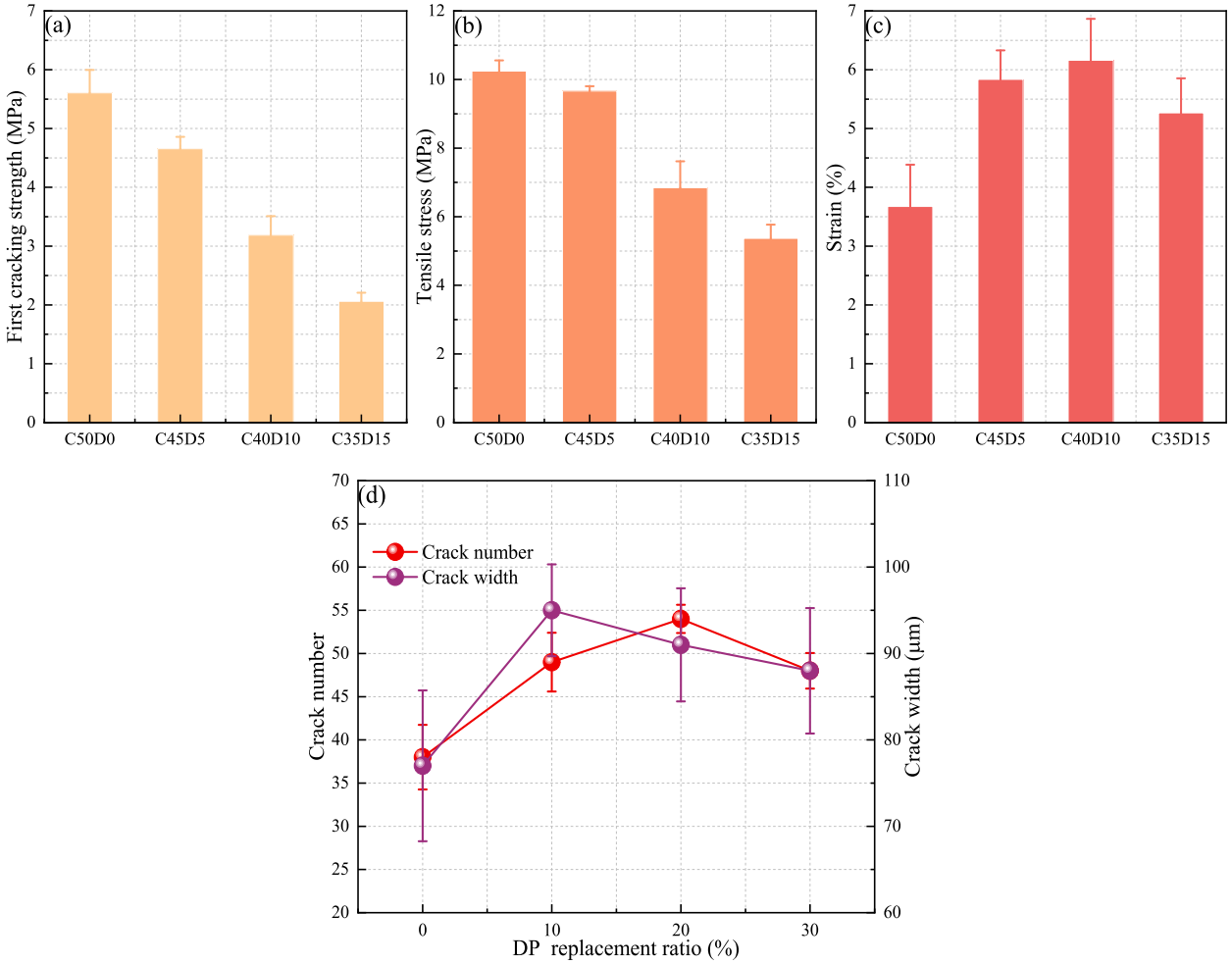

Fig. 9. Tensile parameters of HSECC with different DP replacement ratios. (a) First cracking strength, (b) Ultimate tensile strength, (c) Strain capacity, and (d) Crack parameter.

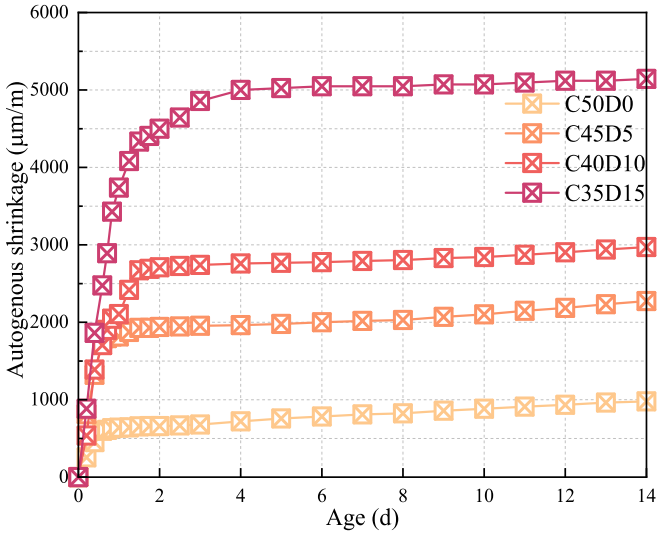

Fig. 10. Autogenous shrinkage of HSECC with various DP contents.

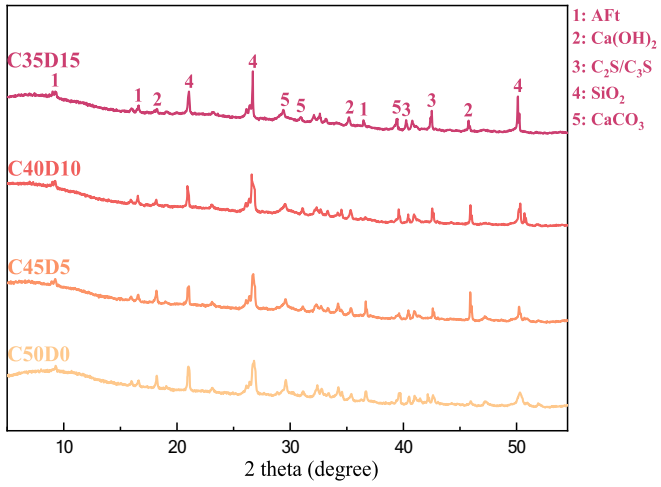

Fig. 11. XRD patterns of HSECC pastes at 28 d.

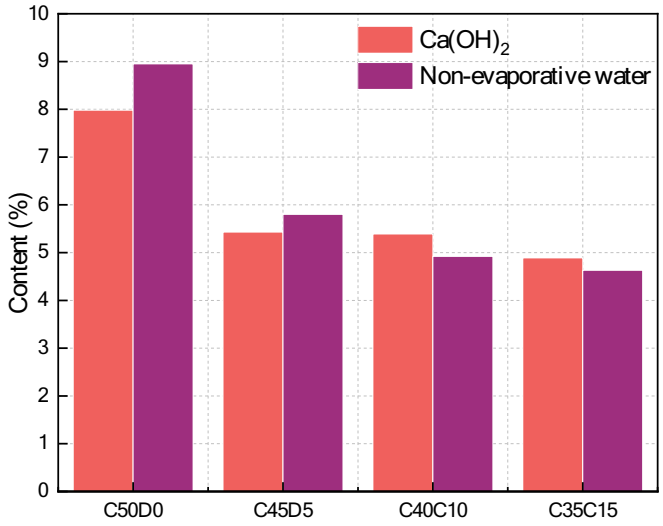

Fig. 13. $Ca(OH)_2$ and non-evaporative water content of paste with DP at 28 d.

water, resulting in decreasing the hydrated degree of cement clinkers at 28 d. With the growth of DP replacement ratio, the peak intensity of SiO_2 gradually increases, which is because that the main chemical component of DP is silicon dioxide (See Fig. 11).

4.4.2. TG

Fig. 12 plots the TG results of paste with DP at 28 d. There are mainly four peaks in the derivative thermogravimetry (DTG) curves, in which the first one ranges from 80 to 130 °C and attributes to the decomposition of AFt and C-S-H gels. The peak of 130–230 °C is due to the dehydration of AFm. The third peak observed at the 400–500 °C is owing to the decomposition of $Ca(OH)_2$. The temperature at the range of 500–780 °C represents the decomposition of $CaCO_3$.

As shown in Fig. 12(a), in the range of 80–230 °C, the weight loss of paste samples with different DP contents are significantly lower than that of the reference sample (C50D0), which shows that the use of DP reduces the content of hydration products, such as AFt and C-S-H gel. This phenomenon corresponds to the change trend of compressive strength with the incorporation of DP. Moreover, the $Ca(OH)_2$ content of each sample is also calculated and ploted in Fig. 13. With increasing DP content, the $Ca(OH)_2$ content of sample gradually reduces. The use of DP instead of cement reduces the content of cement and free water in

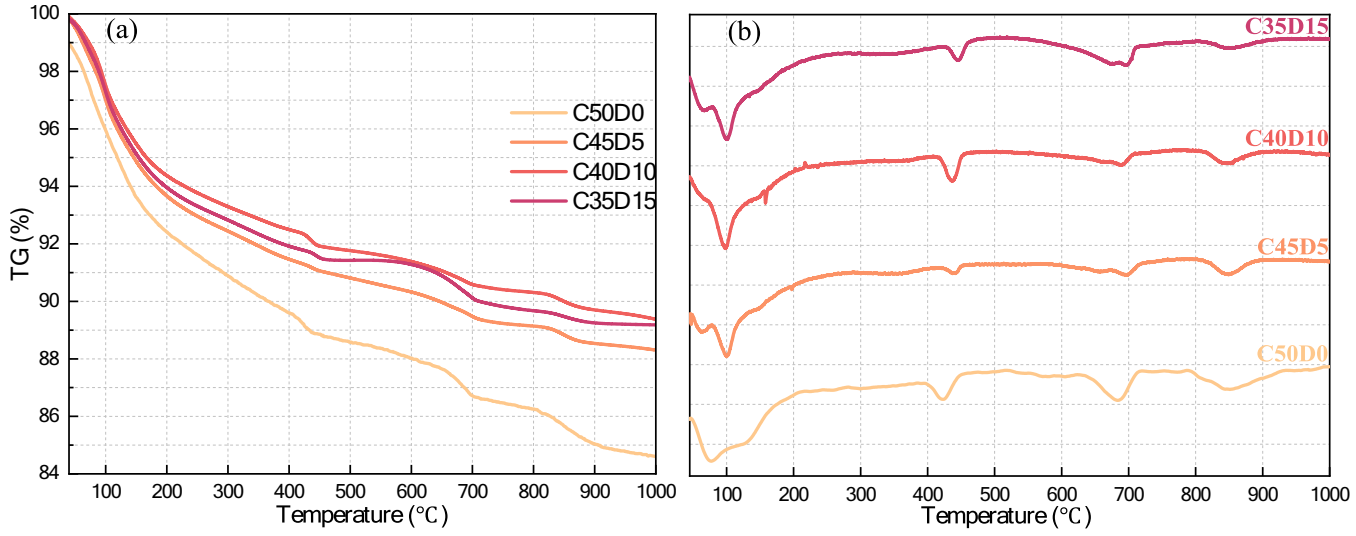

Fig. 12. TG results of paste with DP for 28 d. (a) TG and (b) DTG.

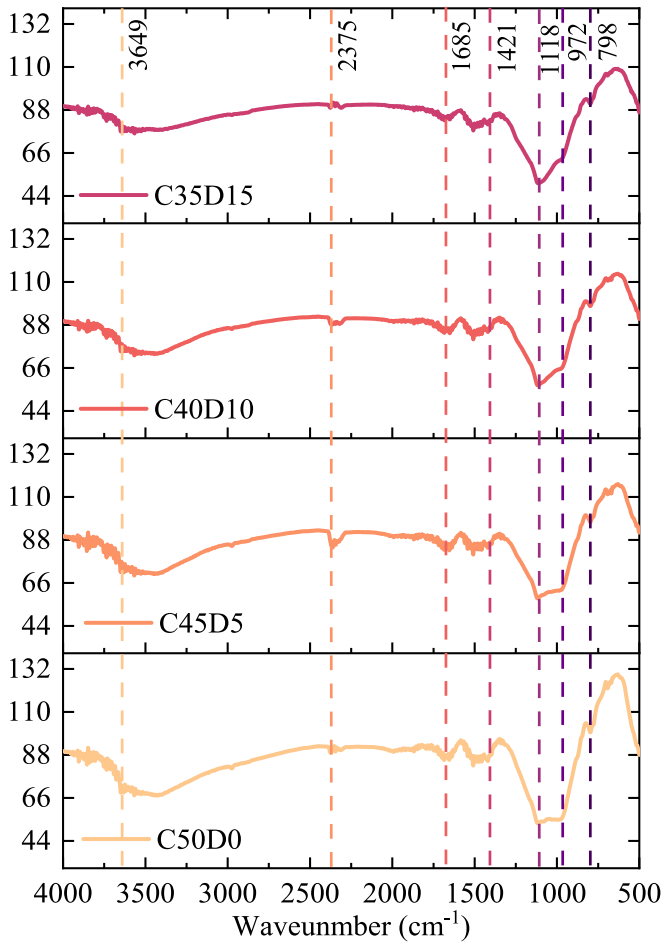

Fig. 14. FT-IR spectra of the paste with different DP contents at 28 d.

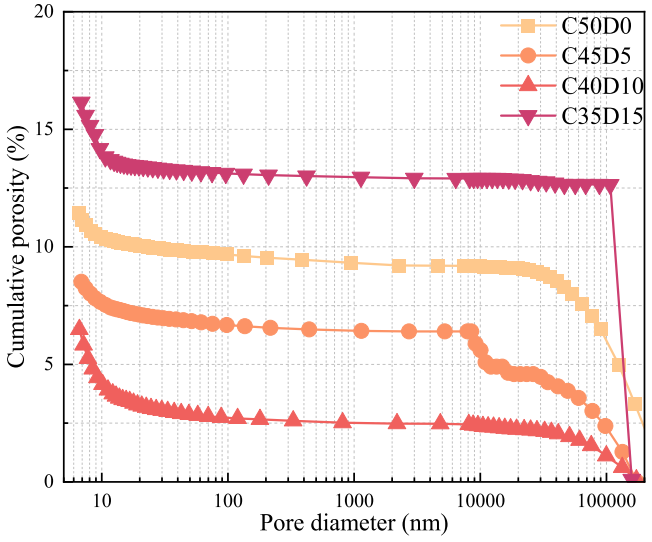

Fig. 15. Cumulative porosity curves of HSECC with different DP contents.

sample, thereby decreasing the amount of hydration products (e.g., $Ca(OH)_2$). Besides, during the hydration process, amorphous silica of the DP particle gradually dissolves and undergoes the pozzolanic reaction, which further consumes $Ca(OH)_2$.

In order to evaluate the reaction degree of the paste, the 28-d non-evaporative water content of the HSECC paste with different DP replacement ratios are also calculated, as plotted in Fig. 13. With increasing the DP replacement ratio, the non-evaporated water content of paste gradually reduces, which implies that the hydration degree of paste reduces. The pozzolanic reaction and internal curing effect of DP contribute to improving hydration degree, but the dilution effect of DP may have a significantly negative influence on the improvement of hydration degree of HSECC paste.

4.4.3. FT-IR

The FT-IR spectra of the paste with different DP contents at 28 d are presented in Fig. 14, which can provide the major characteristic bands of specimens. The band around 3649 cm^{-1} presents the O-H vibration of $Ca(OH)_2$ [40], and the peak shrinks with the increase of DP replacement ratio, verifying that the incorporation of DP reduces the amount of $Ca(OH)_2$. The peak of Si-O can be observed at 798, 972, and 1118 cm^{-1}, which corresponds to the vibration of SiO_2, C-S-H gel, and ettringite, respectively. The wavenumber around 972 and 1118 cm^{-1} reduce with increasing the DP content, indicating that utilizing DP decreases the amount of hydration product (See Fig. 14). The occurrence of peak at 1421 cm^{-1} shows the existence of $CaCO_3$, which associates with the carbonization of $Ca(OH)_2$ during the preparation of sample. The vibration peak of H-O-H is seen at 1685 and 2375 cm^{-1}, which corresponds to the presence of molecular water. In summary, the result of FT-IR certifies that the incorporation of DP reduces the amount of hydration products, which is consistent with the results of XRD and TG test.

4.4.4. MIP

According to the MIP test, the cumulative porosity curves of HSECC with various DP contents are plotted in Fig. 15. Incorporating the DP significantly improves the pore structure of samples because of the filling effect of DP. Compared with reference sample (C50D0) of 11.43%, the porosity of C45D5 and C40D10 samples reduce to 8.79% and 6.71%, respectively. This is mainly because the finer DP particle to replace cement can greatly improve wet packing density of mixture and reduce porosity [41,42]. Meanwhile, the pozzolanic reaction and internal curing effect of DP also contribute to increasing the amount of hydration product, resulting in further increasing the compactness of sample [43]. However, compared with the C40D10 sample of 6.71%, the porosity of C35D15 sample deteriorates and increases to 16.98%. The excessive DP absorbs a large amount of mixing water, which may have a negative effect on the compactness of sample at the age of 28 d. Meanwhile, incorporating excessive DP also dilutes the cement system and may reduce the wet packing density of solid material, which reduces the amount of hydration product and increases the porosity of HSECC sample.

Based on the statement of Zhang et al., there are five types of pore scales in cement-based material, concluding the gel micropore (<10 nm), mesopore (10–50 nm), middle capillary pore (50–100 nm), large capillary pore (100–5000 nm), and macropore (>5000 nm) [44]. It can also be seen from the pore structure characteristic that the incorporation of 0–20% DP causes a decrease in the middle capillary porosity, large capillary porosity and macropore porosity of HSECC, and the gel micropore porosity and mesopore porosity increase (See Fig. 16). Owing to the filling effect of DP, incorporation of an appropriate amount of DP refines the pore structure of sample, which also demonstrates that the use of DP improves the wet packing density of solid particles [45]. Besides, the pozzolanic reaction and internal curing effect of DP also contributes to the refinement of pore structure. However, compared with HSECC with 20% DP, the gel micropore porosity of HSECC with 30% DP increases, whereas the porosity of other types of pore decrease. This indicates that the refinement trends of pores still exist when the DP content increases to 30%. When the DP content increases from 20% to 30%, the macropore porosity of sample increases from 2.47% to 12.91%.

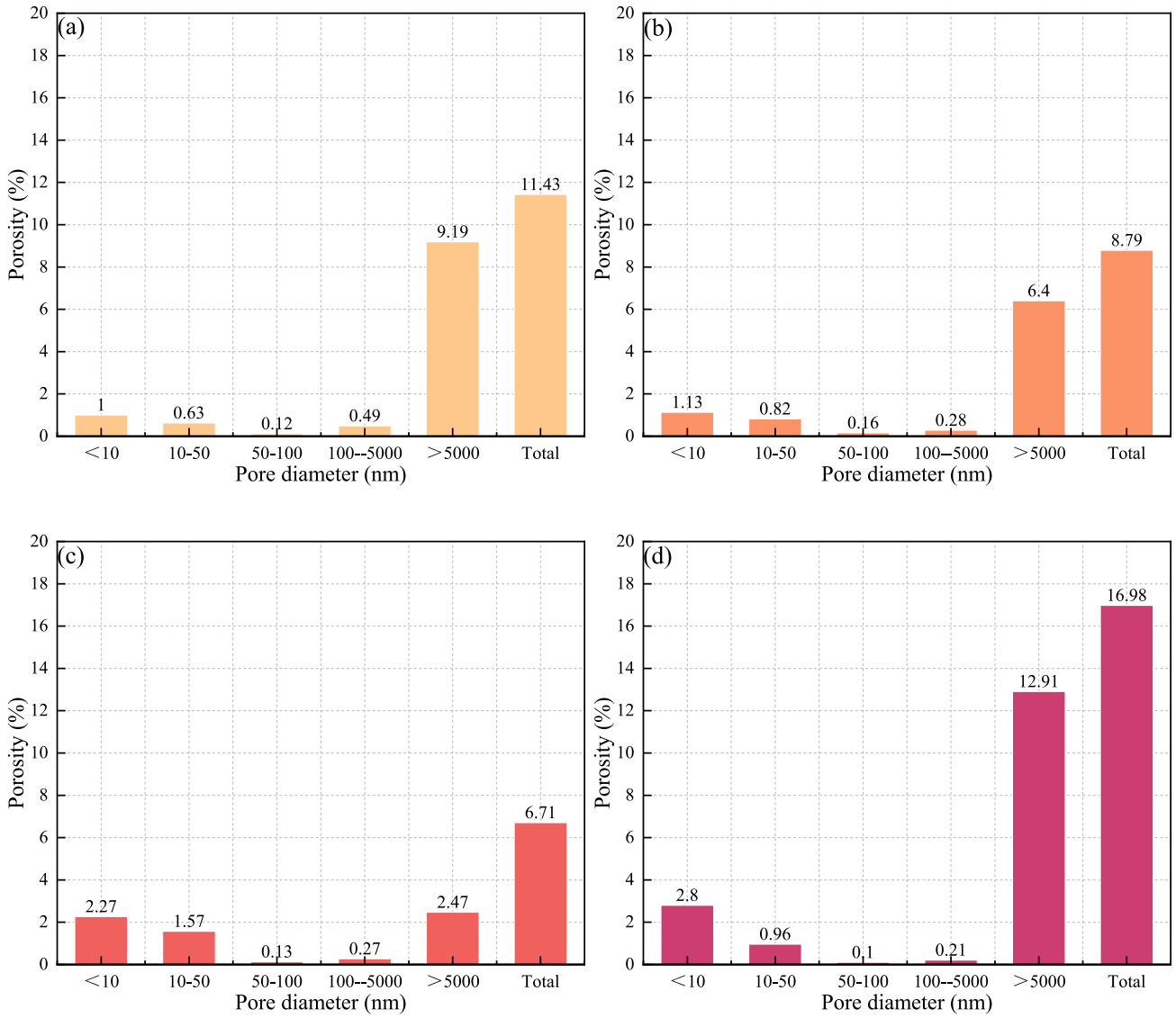

Fig. 16. Pore structure characteristic of HSECC with various DP contents. (a) C50D0, (b) C45D5, (c) C40D10, and (d) C35D15.

4.4.5. SEM

The morphology of fibers in HSECC samples are investigated by the SEM test, and the results are presented in Fig. 17. When the uniaxial tensile loading exceeds the friction force at the fiber/matrix interface, the fibers loose and gradually slip until break, which leaves obvious groove damage on the fiber surface. After tensile test, the damage degree of fiber in the HSECC without DP (C50D0) is severe and there is obvious tearing deformation at fiber ends. For the C50D0 sample, the hydration products of the cementitious material distribute at the fiber/matrix interface, which is beneficial to the improvement of the friction force. Therefore, the fiber ends of C50D0 are seriously damaged after tensile process. With the incorporation of 20% DP, the amount of hydration products of cementitious material decrease, which is not conducive to the friction force at the fiber/matrix interface, resulting in decreasing the ultimate tensile strength of HSECC. Therefore, fibers in HSECC samples containing 20% DP slip more easily from the matrix in comparison with the HSECC without DP (C50D0), which contributes to the improvement of strain-hardening ability of HSECC. After tensile process, the fiber end of the HSECC with 20% DP is flush, which indicates that incorporating DP results in reducing the damage degree of fiber during the tensile process.

4.5. Economic and environmental analysis

The incorporation of DP not only causes the change of mechanical properties, but also affects the economic and environmental benefits of the binder of HSECC. Fig. 18 plots the economic and environmental analysis of binder of HSECC with DP. As a type of solid waste, the DP has a low carbon emission. As the DP dosage increases, the carbon emission of binder in the reference group (C50D0) is 520.1 kg/m^3, while those of the binder with 10%, 20%, 30% DP are 470.1, 420 and 370 kg/m^3, respectively corresponding to approximately 9.6%, 19.2% and 28.9% decrease compared with that of reference group. Meanwhile, the influence of DP replacement ratio on the cost of cementitious material in the HSECC is also similar to that of carbon emission. Total cost of the cementitious material in C35D15 reduces by 10% compared with the reference mixture (C50D0). Therefore, incorporating DP effectively decreases the amount of cement and develops an eco-friendly HSECC with the excellent strain-hardening characteristic.

5. Conclusion

In this study, a series of experiments and assessment are systematically performed to study the high volume of SCM on the mechanical

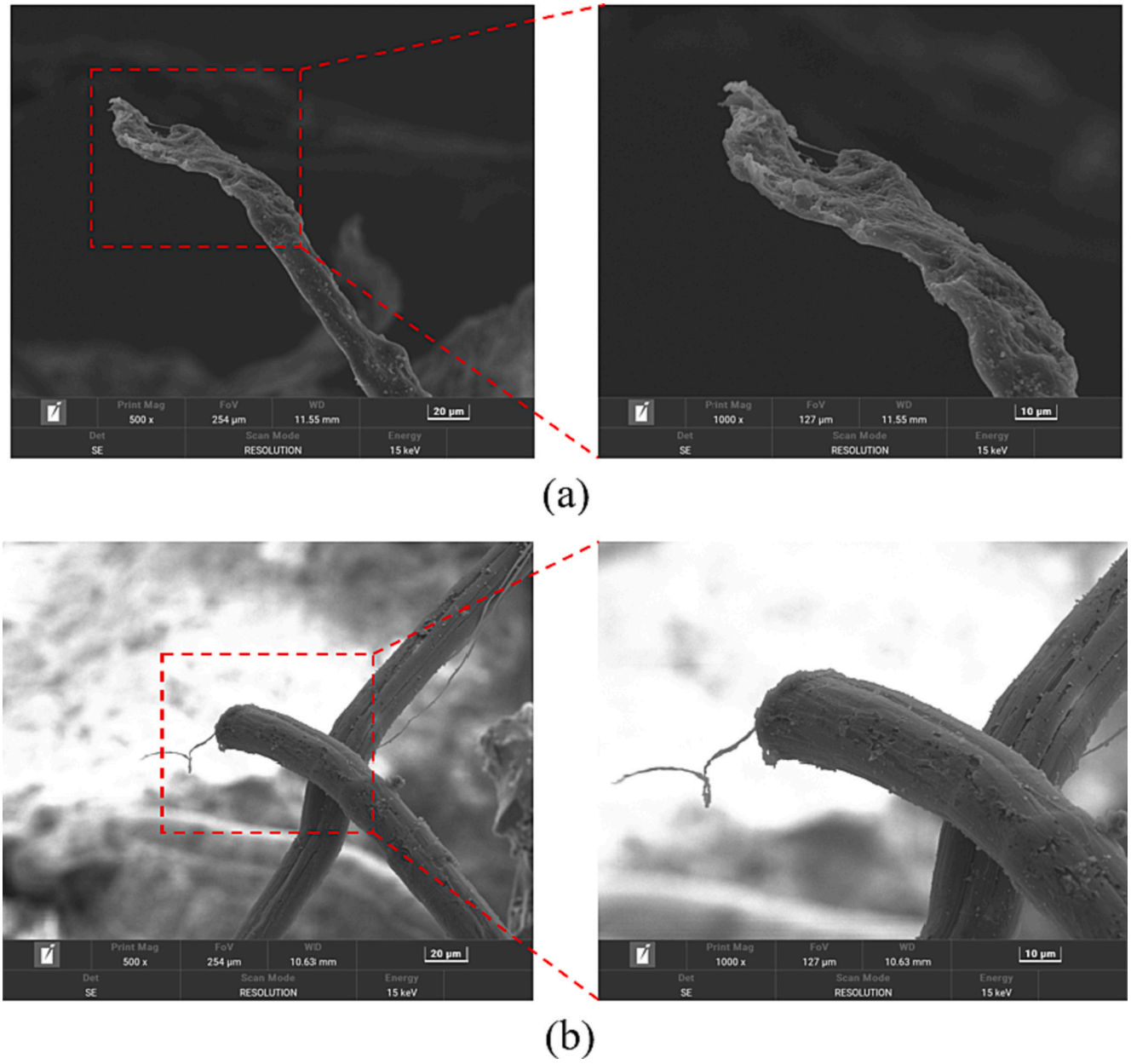

Fig. 17. SEM image of fiber ends. (a) C50D0 and (b) C40D10.

properties, autogenous shrinkage, and microstructure of HSECC. Incorporating high-volume SCM in the ECC system is beneficial to prepare the eco-friendly ECC. The key conclusions are listed as follows.

(1) Although the incorporation of DP decreases the compressive strength of HSECC, the 28-d compressive strength of HSECC containing 10% DP still reaches the 81.74% of the reference sample.
(2) The effect of DP content on the first cracking strength and ultimate tensile strength is similar to the compressive strength, which gradually decreases with the increase of DP replacement ratio. Nevertheless, the strain capacity of HSECC increases with the DP content up to 20% and then slightly reduces. Excessive DP replacing cement may have a significantly negative influence on the improvement of fiber-bridge stress of HSECC, which is harmful to the improvement of strain capacity.
(3) As the DP replacement ratio increases, the autogenous shrinkage of HSECC gradually increases, which may be mainly due to the reduction of stiffness and effective water-binder ratio in sample.
(4) Using DP instead of cement decreases the $Ca(OH)_2$ content, and brings an amount of SiO_2 into the HSECC sample. With the increase of DP content, the porosity of gel micropore and mesopore increase but the pore size of sample tends to be finer. Meanwhile, incorporating DP also reduces the non-evaporative water content, which indicates the incorporation of DP reduces the hydration degree of HSECC system.
(5) The carbon emission and cost of binder in HSECC decrease with the increase of DP content, which reduces the huge environmental impact caused by cement production and expands the application of DP in civil engineering. Compared with the HSECC without DP, the carbon emission and cost of binder in the HSECC with 30% DP reduce by 28.9% and 10%, respectively.

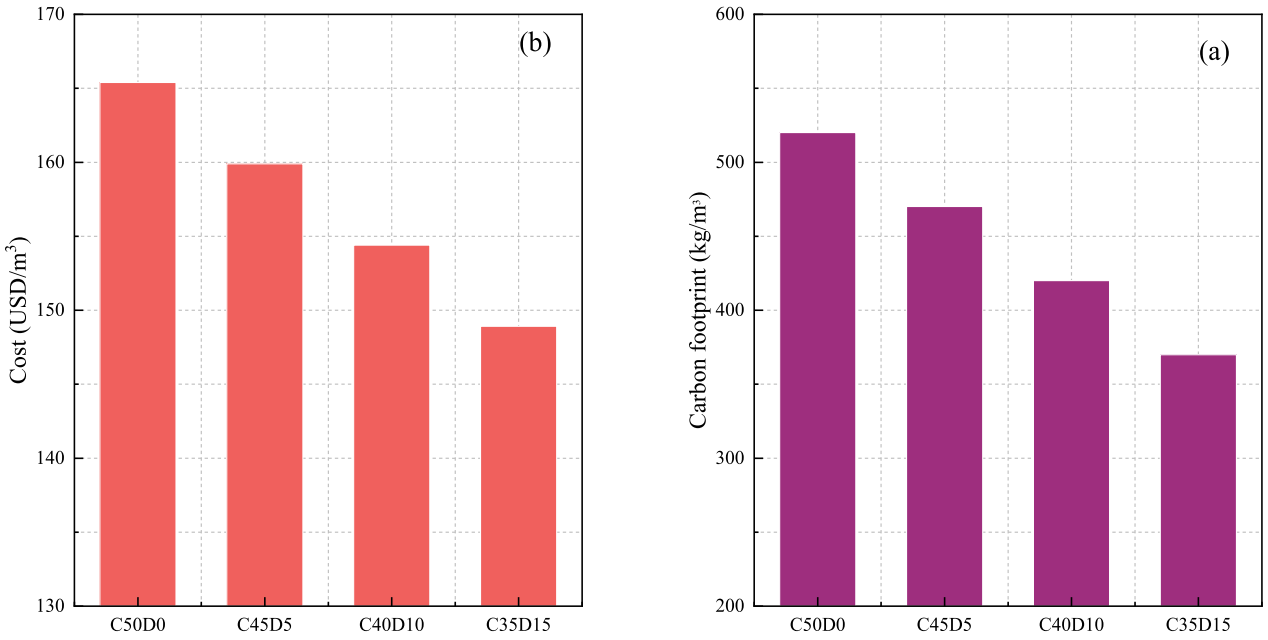

Fig. 18. Economic and environmental analysis results of cementitious material in the HSECC mixed with DP. (a) Cost and (b) Carbon footprint.

CRediT authorship contribution statement

Minghu Zhang: Investigation, Formal analysis, Writing – original draft. **Xuezhen Zhu:** Validation, Writing – review & editing. **Sukhoon Pyo:** Methodology, Writing – review & editing. **Yuanxia Yang:** Conceptualization, Writing – review & editing. **Baoju Liu:** Conceptualization, Writing – review & editing. **Jinyan Shi:** Methodology, Writing – review & editing.

Declaration of Competing Interest

None.

Data availability

Data will be made available on request.

Acknowledgments

The authors would like to thank the financial supports from the Science and Technology Research and Development Program Project of China Railway Group Limited (Key Project, No.: 2021-Key-08).

References

[1] G. Kaplan, O.Y. Bayraktar, T. Bayraktar, Optimization of without SCM concrete exposed to seawater according to minimum cost and CO_2 emissions: sustainable design with ABC algorithm, Mater. Today Commun. 35 (2023), 105657.
[2] G. Kaplan, O.Y. Bayraktar, B. Bayrak, O. Celebi, B. Bodur, A. Oz, A.C. Aydin, Physico-mechanical, thermal insulation and resistance characteristics of diatomite and attapulgite based geopolymer foam concrete: effect of different curing regimes, Constr. Build. Mater. 373 (2023), 130850.
[3] H. Du, K.H. Tan, Properties of high volume glass powder concrete, Cement Concrete Comp. 75 (2017) 22–29.
[4] J. Liu, M.U. Hossain, S.T. Ng, H. Ye, High-performance green concrete with high-volume natural pozzolan: mechanical, carbon emission and cost analysis, J. Build. Eng. 68 (2023), 106087.
[5] H.M. Hamada, A.A.A. Al-attar, F.M. Yahaya, K. Muthusamy, B.A. Tayeh, A. M. Humada, Effect of high-volume ultrafine palm oil fuel ash on the engineering and transport properties of concrete, Case Stud. Constr. Mat. 12 (2020), e318.
[6] H.S. Gökçe, B.C. Öztürk, N.F. Çam, Ö. Andiç-Çakır, Gamma-ray attenuation coefficients and transmission thickness of high consistency heavyweight concrete containing mineral admixture, Cement Concrete Comp. 92 (2018) 56–69.
[7] M.N.A.A. Aeshah, G. Kaplan, Mechanical durability and microstructural properties of sustainable high strength mortars incorporated basalt fiber and copper slag: Taguchi optimization, Constr. Build. Mater. 339 (2022), 127815.
[8] B. Xi, Y. Zhou, K. Yu, B. Hu, X. Huang, L. Sui, F. Xing, Use of nano-SiO_2 to develop a high performance green lightweight engineered cementitious composites containing fly ash cenospheres, J. Clean. Prod. 262 (2020), 121274.
[9] V.C. Li, C.K.Y. Leung, Steady-state and multiple cracking of short random fiber composites, J. Eng. Mech. 11 (1992) 2246–2264.
[10] J. Kim, J. Kim, G.J. Ha, Y.Y. Kim, Tensile and fiber dispersion performance of ECC (engineered cementitious composites) produced with ground granulated blast furnace slag, Cem. Concr. Res. 37 (2007) 1096–1105.
[11] V.C. Li, S. Wang, C. Wu, Tensile strain-hardening behavior of polyvinyl alcohol engineered cementitious composite (PVA-ECC), Dent. Mater. J. 98 (6) (2001) 483–492.
[12] W. Yuan, Q. Han, Y. Bai, X. Du, Z. Yan, Compressive behavior and modelling of engineered cementitious composite (ECC) confined with LRS FRP and conventional FRP, Compos. Struct. 272 (2021), 114200.
[13] J.D. Wu, L.P. Guo, Y.Z. Cao, et al., Mechanical and fiber/matrix interfacial behavior of ultra-high-strength and high-ductility cementitious composites incorporating waste glass powder, Cement Concrete Comp. 126 (2022), 104371.
[14] Y. Zhu, Z. Zhang, Y. Yang, Y. Yao, Measurement and correlation of ductility and compressive strength for engineered cementitious composites (ECC) produced by binary and ternary systems of binder materials: Fly ash, slag, silica fume and cement, Constr. Build. Mater. 68 (2014) 192–198.
[15] M. Şahmaran, V.C. Li, Durability properties of micro-cracked ECC containing high volumes fly ash, Cem. Concr. Res. 39 (2009) 1033–1043.
[16] H. Ma, S. Qian, Z. Zhang, Z. Lin, V.C. Li, Tailoring engineered cementitious composites with local ingredients, Constr. Build. Mater. 101 (2015) 584–595.
[17] J. Wu, L. Guo, Y. Qin, Preparation and characterization of ultra-high-strength and ultra-high-ductility cementitious composites incorporating waste clay brick powder, J. Clean. Prod. 312 (2021), 127813.
[18] Z. Zhang, F. Yang, J. Liu, S. Wang, Eco-friendly high strength, high ductility engineered cementitious composites (ECC) with substitution of fly ash by rice husk ash, Cem. Concr. Res. 137 (2020), 106200.
[19] Z. Ahmadi, J. Esmaeili, J. Kasaei, R. Hajialioghli, Properties of sustainable cement mortars containing high volume of raw diatomite, Sustain. Mater. Technol. 16 (2018) 47–53.
[20] D. Kastis, G. Kakali, S. Tsivilis, M.G. Stamatakis, Properties and hydration of blended cements with calcareous diatomite, Cem. Concr. Res. 36 (2006) 1821–1826.
[21] M. Sarıdemir, S. Çelikten, A. Yıldırım, Mechanical and microstructural properties of calcined diatomite powder modified high strength mortars at ambient and high temperatures, Adv. Powder Technol. 31 (2020) 3004–3017.
[22] M. Sun, C. Zou, D. Xin, Pore structure evolution mechanism of cement mortar containing diatomite subjected to freeze-thaw cycles by multifractal analysis, Cement Concrete Comp. 114 (2020), 103731.
[23] H.H. Wong, A.K. Kwan, Packing density of cementitious materials: Part 1—measurement using a wet packing method, Mater. Struct. 41 (2008) 689–701.
[24] A.K. Kwan, H.H.C. Wong, Packing density of cementitious materials: Part 2—packing and flow of OPC+ PFA+ CSF, Mater. Struct. 41 (2008) 773–784.
[25] M. Lai, L. Hanzic, J.C. Ho, Fillers to improve passing ability of concrete, Struct. Concr. 20 (1) (2019) 185–197.

[26] H. Baloch, M. Usman, S.A. Rizwan, A. Hanif, Properties enhancement of super absorbent polymer (SAP) incorporated self-compacting cement pastes modified by nano silica (NS) addition, Constr. Build. Mater. 203 (2019) 18–26.
[27] C.S. Poon, L. Lam, Y.L. Wong, A study on high strength concrete prepared with large volumes of low calcium fly ash, Cem. Concr. Res. 30 (2000) 447–455.
[28] Y. Nie, J. Shi, Z. He, B. Zhang, Y. Peng, J. Lu, Evaluation of high-volume fly ash (HVFA) concrete modified by metakaolin: technical, economic and environmental analysis, Powder Technol. 397 (2022), 117121.
[29] H.S. Müller, M. Haist, M. Vogel, Assessment of the sustainability potential of concrete and concrete structures considering their environmental impact, performance and lifetime, Constr. Build. Mater. 67 (2014) 321–337.
[30] Z. He, X. Han, M. Zhang, Q. Yuan, J. Shi, P. Zhan, A novel development of green UHPC containing waste concrete powder derived from construction and demolition waste, Powder Technol. 398 (2022), 117075.
[31] P.S.M. Thilakarathna, S. Seo, K.S.K. Baduge, H. Lee, P. Mendis, G. Foliente, Embodied carbon analysis and benchmarking emissions of high and ultra-high strength concrete using machine learning algorithms, J. Clean. Prod. 262 (2020), 121281.
[32] T. Saidi, M. Hasan, The effect of partial replacement of cement with diatomaceous earth (DE) on the compressive strength and absorption of mortar, J. King Saud Univ. Eng. Sci. 34 (2022) 250–259.
[33] Y. Zhou, G. Gong, B. Xi, M. Guo, F. Xing, C. Chen, Sustainable lightweight engineered cementitious composites using limestone calcined clay cement (LC^3), Compos. Part B-Eng. 243 (2022), 110183.
[34] Q. Wang, M.H. Lai, J. Zhang, Z. Wang, J.C.M. Ho, Greener engineered cementitious composite (ECC)–the use of pozzolanic fillers and unoiled PVA fibers, Constr. Build. Mater. 247 (2020), 118211.
[35] Y. Zhu, Y. Yang, Y. Yao, Use of slag to improve mechanical properties of engineered cementitious composites (ECCs) with high volumes of fly ash, Constr. Build. Mater. 36 (2012) 1076–1081.
[36] D. Lei, L. Guo, Y. Li, Z. Zheng, J. Liu, S. Li, P. Wang, C. Li, V. Mechtcherine, Z. Li, D. Zeng, B. Zhong, The investigating on mechanical properties of ultra-high strength and ultra-high ductility cementitious composites (UHS-UHDCC), J. Build. Eng. 43 (2021), 102486.
[37] H.A. Mesbah, F. Buyle-Bodin, Efficiency of polypropylene and metallic fibres on control of shrinkage and cracking of recycled aggregate mortars, Constr. Build. Mater. 13 (1999) 439–447.
[38] M.H. Lai, S.A.M. Binhowimal, A.M. Griffith, L. Hanzic, Z. Chen, Q. Wang, J.C. M. Ho, Shrinkage, cementitious paste volume, and wet packing density of concrete, Struct. Concr. 23 (1) (2022) 488–504.
[39] M.H. Lai, S.A.M. Binhowimal, A.M. Griffith, L. Hanzic, Q. Wang, Z. Chen, J.C. M. Ho, Shrinkage design model of concrete incorporating wet packing density, Constr. Build. Mater. 280 (2021), 122448.
[40] H. Wang, G. Long, Y. Xie, X. Zeng, K. Ma, R. Dong, Z. Tang, Q. Xiao, Effects of intense ultraviolet irradiation on drying shrinkage and microstructural characteristics of cement mortar, Constr. Build. Mater. 347 (2022), 128513.
[41] L. Hanzic, J.C.M. Ho, Multi-sized fillers to improve strength and flowability of concrete, Adv. Cem. Res. 29 (3) (2017) 112–124.
[42] B.A. Kounakoff, L. Hanzic, J.C.M. Ho, Limestone and silica fume to improve concurrent flowability–segregation limits of concrete, Mag. Concr. Res. 69 (23) (2017) 1189–1202.
[43] Q. Fu, X. Zhao, Z. Zhang, W. Xu, D. Niu, Effects of nanosilica on microstructure and durability of cement-based materials, Powder Technol. 117447 (2022).
[44] L. Zhang, G. Lin, X. Qian, D. Yan, K. Qian, S. Ruan, Unveil the role of nano-$CaCO_3$ in early shrinkage and tensile properties of cement paste: from experimental work to modeling, Compos. Part B: Eng. 243 (2022), 110185.
[45] S.H. Chu, W.L. Lam, L. Li, C.S. Poon, Packing density of ternary cementitious particles based on wet packing method, Powder Technol. 405 (2022), 117493.